



HAL
open science

Ionic-to-Electronic Conductivity Crossover in CdTe-AgI-As₂Te₃ Glasses An 110mAg Tracer Diffusion Study

M. Kassem, I. Alekseev, M. Bokova, David Le Coq, E. Bychkov

► **To cite this version:**

M. Kassem, I. Alekseev, M. Bokova, David Le Coq, E. Bychkov. Ionic-to-Electronic Conductivity Crossover in CdTe-AgI-As₂Te₃ Glasses An 110mAg Tracer Diffusion Study. *Journal of Physical Chemistry B*, 2018, 122 (14), pp.4179-4186. 10.1021/acs.jpcc.8b00739 . hal-01809150

HAL Id: hal-01809150

<https://univ-rennes.hal.science/hal-01809150v1>

Submitted on 19 Jun 2018

HAL is a multi-disciplinary open access archive for the deposit and dissemination of scientific research documents, whether they are published or not. The documents may come from teaching and research institutions in France or abroad, or from public or private research centers.

L'archive ouverte pluridisciplinaire **HAL**, est destinée au dépôt et à la diffusion de documents scientifiques de niveau recherche, publiés ou non, émanant des établissements d'enseignement et de recherche français ou étrangers, des laboratoires publics ou privés.

Ionic-to-Electronic Conductivity Crossover in CdTe-AgI-As₂Te₃ Glasses: An ^{110m}Ag Tracer Diffusion Study

M. Kassem,^{*,1} I. Alekseev,² M. Bokova,¹ D. Le Coq,³ and E. Bychkov¹

¹LPCA, Université du Littoral Côte d'Opale ULCO, LPCA, EA CNRS 4493, F-59140 Dunkerque, France

²V.G. Khlopin Radium Institute, 194021 St. Petersburg, Russia

³Sciences Chimiques de Rennes, Univ. de Rennes I, 35042 Rennes, France

*E-mail: Mohamad.Kassem@univ-littoral.fr. Phone: +33-328-658270.

ABSTRACT

Conductivity isotherms of (CdTe)_x(AgI)_{0.5-x/2}(As₂Te₃)_{0.5-x/2} glasses (0.0 ≤ x ≤ 0.15) reveal a non-monotonic behavior with increasing CdTe content reminiscent of mixed cation effect in oxide and chalcogenide glasses. Nevertheless, the apparent similarity appears to be partly incorrect. Using ^{110m}Ag tracer diffusion measurements, we show that semiconducting CdTe additions produce a dual effect: (i) decreasing the Ag⁺ ion transport by a factor of ≈200 with a simultaneous increase of the diffusion activation energy, and (ii) increasing the electronic conductivity by 1.5 orders of magnitude. Consequently, the conductivity minimum at x = 0.05 reflects an ionic-to-electronic transport crossover; the silver ion transport number decreases by three orders of magnitude with increasing x.

1. INTRODUCTION

Tracer diffusion experiments have been widely used in the past to study ion transport in oxide glasses.¹⁻⁴ Among the most important results found previously, we should note: (i) the diffusion coefficients of alkali cations are significantly higher than those of alkaline-earth ions, oxygen species, or glass-forming elements (Si, Al ...); (ii) a diffusivity crossover in the mixed alkali glasses; (iii) the Haven ratio H_R varies systematically, $0.2 \leq H_R \leq 1$, depending on the mobile ion content. Nevertheless, until recently, diffusion measurements in chalcogenide glasses were rather scarce.⁵⁻⁷ However, during the last decade, several diffusion studies combining both electrical conductivity and radioactive tracer diffusion D^* were presented; thus highlighting phenomena that could not be reached by electrical measurements alone.⁸⁻¹⁴

Recently, chalcogenide glasses in the ternary system CdTe-AgI-As₂Te₃¹⁵ were synthesized, and the effect of CdTe semiconductor additives on transport and physical properties of binary AgI-As₂Te₃ glasses has been investigated.^{16,17} The glass-forming range for (CdTe)_x(AgI)_{0.5-x/2}(As₂Te₃)_{0.5-x/2} compositions was found to be limited to $x \leq 0.15$. The glass transition temperature T_g decreases in the range $0.0 \leq x \leq 0.1$ and remains constant with further increasing x . More importantly, the electrical properties of cadmium telluride glasses exhibit a non-monotonic behavior with (i) diminished ($x \leq 0.05$) and (ii) enhanced total conductivity σ_{dc} ($x > 0.05$), reminiscent of mixed cation effect in oxide and chalcogenide glasses. Semiconducting CdTe additions were assumed to produce two distinct phenomena: (i) a decrease of the ionic conductivity by blocking the Ag⁺ ion transport within the preferential conduction pathways, and (ii) an increase of the electronic conductivity caused by Te 5p lone-pair electronic states in the top of the valence band.

The present paper deals with ^{110m}Ag tracer diffusion measurements in the ternary (CdTe)_x(AgI)_{0.5-x/2}(As₂Te₃)_{0.5-x/2} glasses, which would allow to obtain a detailed information on the ionic and electronic components of the charge transport.

2. EXPERIMENTAL DETAILS

2.1 Glass Preparation

(CdTe)_x(AgI)_{0.5-x/2}(As₂Te₃)_{0.5-x/2} samples ($x = 0, 0.01, 0.025, 0.05, 0.075, 0.10, 0.125, 0.15, 0.17, 0.20$) were prepared using the appropriate proportions of CdTe, AgI and As₂Te₃. The starting materials were sealed under vacuum (10^{-6} mbar) in a cleaned silica tube (8 mm ID and 1 mm wall thickness), heated slowly in a rocking furnace to 850 °C at 5 K min⁻¹ heating rate, maintained at this temperature for 24 hours, then cooled down to 650 °C before quenching in cold salt/water mixture. Several three-gram samples were obtained for each composition. Further synthesis details and properties characteristic to this telluride system are published elsewhere.¹⁵

2.2 Conductivity Measurements

Total electrical conductivity of the samples was measured using a Hewlett Packard 4194A impedance meter. The impedance modulus Z and the phase angle θ were obtained in the frequency range from 100 Hz to 15 MHz at temperatures between 293 and 378 K, the maximum temperature was below T_g for the glass samples.¹⁹ The quenched samples, prepared as rectangular plates, were polished using SiC powder (9.3 μ grain size). The sample sides were ground parallel and gold was deposited on opposite sides to form electrodes for conductivity experiment, i.e., the electrochemical cell for conductivity measurements was Au|glass|Au. Typical thickness and area of the samples were in the range of 0.7-1.5 mm and 6-8 mm², respectively. Further details of conductivity measurements are published previously.¹⁵⁻¹⁸

2.3 ^{110m}Ag Tracer Experiments

The ^{110m}Ag tracer (the half-life $t_{1/2} = 249.76$ d) was produced by the ¹⁰⁹Ag(n,γ)^{110m}Ag nuclear reaction in a research reactor of St. Petersburg Nuclear Physics Institute using thermal neutrons with an average flux of $8.0(2) \times 10^{13}$ n cm⁻² s⁻¹. For each composition, samples having the same conductivity parameters within the experimental uncertainty were used in diffusion experiments. Measurements were carried out using thin-layer geometry. A drop of radioactive ^{110m}AgNO₃ solution was deposited onto one face of the sample, kept there for 2 h, wiped with a filter paper, washed with distilled water and ethyl alcohol, and then dried. The sample was wrapped in aluminium foil and encapsulated in a Pyrex tube. The samples were annealed in a furnace at 20 to 115 °C for a period of several hours to 60 days. The diffusion anneals were terminated by quenching the samples in air. The sides of the sample parallel to the diffusion direction were ground to eliminate surface diffusion effects. The sample was then sectioned on a parallel grinder. The thickness of each section was determined either from the density, cross-sectional area and weight change of the sample, or by direct thickness measurements. In the latter case, the thickness uncertainty was ± 5 μ m. Further details on tracer diffusion measurements were published elsewhere.¹⁹

3. RESULTS AND DISCUSSION

3.1 Tracer Diffusion Results

Penetration profiles for ^{110m}Ag tracer diffusion in the CdTe-AgI-As₂Te₃ glasses obey the usual solution of Fick's law for an infinitesimally thin deposit of radioactive isotope on a semi-infinite specimen²:

$$1 - \frac{A(y,t)}{A_0} = \text{erf}(q), \quad (1)$$

where

$$q = \frac{y}{2\sqrt{D_{\text{Ag}}t}}, \quad (2)$$

$A(y,t)$ is the residual activity of the sample after a thickness y was removed, t is the diffusion anneal time, A_0 is the initial residual activity, D_{Ag} is the tracer diffusion coefficient, and $\text{erf}(q)$ is the Gauss error function. Experimentally determined values of $A(y,t)$ and A_0 yield q values which, when plotted vs. y , produce a straight line passing through the origin, Figure 1.

The silver tracer diffusion coefficients D_{Ag} , determined from the slope of the penetration profiles, are given in Figure 2, plotted as $\log D_{\text{Ag}}$ versus T^{-1} . Figure 2 shows that the temperature dependences of the tracer diffusion coefficient are in good agreement with Arrhenius-type activation dependence

$$D = D_0 \exp\left(-\frac{E_d}{kT}\right), \quad (3)$$

where D_0 is the diffusion pre-exponential factor, E_d the diffusion activation energy, k and T have their usual meaning. The derived diffusion parameters D_{298} , E_d and D_0 were calculated from a least-square fit of the data to Equation (3). D_{298} corresponds to room-temperature silver tracer diffusion coefficient D_{Ag} . The results are listed in Table 1 and shown in Figure 3.

The $^{110\text{m}}\text{Ag}$ tracer diffusion coefficient decreases monotonically by 2.3 orders of magnitude with increasing x from $6.8 \times 10^{-11} \text{ cm}^2 \text{ s}^{-1}$ ($x = 0$) to $3.8 \times 10^{-13} \text{ cm}^2 \text{ s}^{-1}$ ($x = 0.15$) at room temperature (Table 1). Fig. 3a shows that the conductivity and tracer diffusion isotherms for the ternary CdTe-AgI-As₂Te₃ glasses are significantly different, especially at $x \geq 0.05$. These results are consistent with our previous assumption¹⁹ that the ternary glasses, depending on x , are either mixed or predominantly electronic conductors. Fig. 3b shows that the diffusion activation energy E_d increases simultaneously from 0.47 eV to 0.68 eV. Meanwhile, the pre-exponential factor D_0 increases by a factor of 15 with increasing x , Fig. 3c. Similar increase of D_0 was also observed in the $(\text{CdSe})_x(\text{AgI})_{0.5-x/2}(\text{As}_2\text{Se}_3)_{0.5-x/2}$ system.¹⁹ The diffusion pre-exponential factor is proportional to the attempt frequency ν_0 , the jump distance ℓ , and the activation entropy for the jump of a mobile ion ΔS^\ddagger

$$D_0 \propto \nu_0 \ell^2 \exp(\Delta S^\ddagger/k), \quad (4)$$

where k is the Boltzmann constant. Neglecting the entropy term, the D_0 increase may be related either to higher ν_0 , or to longer ℓ . Taking into account the proposed immobilization of some Ag⁺ cations by cadmium species within the preferential conduction pathways in the CdSe-AgI-As₂Se₃ glasses¹⁹, the effective jump distance is expected to increase with x , thus increasing D_0 .

3.2 Apparent Haven Ratio

The Haven ratio H_R is a simple experimental parameter easily accessible from a combined (tracer diffusion coefficient D and ionic conductivity σ_i) experiment or from a single electro-diffusion or Chemla measurement. Since the total conductivity σ_{dc} , measured using impedance spectroscopy, is not purely ionic, i.e., the silver ion transport number $t_{Ag^+} < 1$, we cannot calculate the Haven ratio H_R ²⁰

$$H_R = \frac{D_{Ag}}{D_\sigma}, \quad (5)$$

where D_σ is the conductivity diffusion coefficient calculated from the ionic conductivity σ_i using the Nernst-Einstein relation

$$D_\sigma = \frac{kT\sigma_i}{N(ze)^2}, \quad (6)$$

where N is the concentration of the mobile species, ze is the electric charge of the carrier ion, and k and T have their usual meaning. However, we have calculated the apparent Haven ratio $t_{Ag^+}H_R$ using the usual definition of the ion transport number

$$\sigma_i = t_{Ag^+} \sigma_{dc} \quad (7)$$

By combining the equations 5, 6 and 7, the apparent Haven ratio $t_{Ag^+}H_R$ can be expressed as:

$$t_{Ag^+}H_R = \frac{D_{Ag}N(ze)^2}{kT\sigma} \quad (8)$$

The calculated $t_{Ag^+}H_R$ are presented in Figure 4 as a function of temperature and their average values are also given in Table 1. The apparent Haven ratio decreases significantly with x from $t_{Ag^+}H_R = 0.16 \pm 0.02$ for the $x = 0$ glassy host, $(AgI)_{0.5}(As_2Te_3)_{0.5}$, to $t_{Ag^+}H_R = (3.7 \pm 0.8) \times 10^{-4}$ for the $x = 0.15$ glass at the limit of the glass-forming range. Since the overall changes of the Haven ratio in glasses and crystals are limited, $0.2 \leq H_R \leq 1$ (see for example, references^{1,2,8,17,20} and references therein), doping with CdTe results in a remarkable decrease of t_{Ag^+} , at least by two or three orders of magnitude, discussed in details in the next section.

3.3 Ionic versus Electronic Transport

Analysis of the total conductivity σ_{dc} and ^{110m}Ag tracer diffusion D_{Ag} allows the ionic and electronic transport to be distinguished. Figure 5a shows the room-temperature conductivity σ_{dc} and its ionic counterpart $H_R\sigma_{Ag^+}$, calculated from D_{Ag} using Equations (5)

and (6). The two activation energies and pre-exponential factors are compared in Fig. 5b and Fig. 5c.

A non-monotonic change in σ_{dc} accompanied by a shallow maximum in the conductivity activation energy E_{σ} seems to be related to a crossover from the mixed conducting glasses with a significant contribution of the Ag^+ ion transport to the CdTe-rich vitreous alloys having predominantly electronic conductivity. Similar phenomenon was observed in the binary $(\text{AgI})_z(\text{As}_2\text{Te}_3)_{1-z}$ glassy system with variable silver iodide content z .^{16,17} The AgI-poor glasses are essentially electronic conductors but the Ag^+ ion transport becomes predominant at $z \geq 0.4$. The most concentrated $(\text{AgI})_{0.6}(\text{As}_2\text{Te}_3)_{0.4}$ and $(\text{AgI})_{0.8}(\text{As}_2\text{Te}_3)_{0.2}$ glasses appear to be nearly pure ionic conductors with $t_{\text{Ag}^+} \cong 1$ and $t_{\text{Ag}^+} \gg t_e$, where $t_e = t_n + t_p$ is the electron transport number of n - and/or p -type.¹⁷ Using the apparent Haven ratio $t_{\text{Ag}^+}H_R$ for the ternary glasses, we can estimate the silver ion transport numbers t_{Ag^+} in this system. The Haven ratio for the ion-conducting glass $(\text{AgI})_{0.6}(\text{As}_2\text{Te}_3)_{0.4}$, $H_R = 0.44 \pm 0.08$, is very similar to those for AgI-rich superionic $(\text{AgI})_z(\text{As}_2\text{Se}_3)_{1-z}$ vitreous alloys, $H_R = 0.40 \pm 0.04$ at $z \geq 0.4$.^{17,19} Assuming that the $(\text{AgI})_{0.5}(\text{As}_2\text{Te}_3)_{0.5}$ glass also has $H_R = 0.44$, the calculated t_{Ag^+} values vary between 0.8 and 0.2 for this particular composition, Figure 6.

The observed decrease of t_{Ag^+} with increasing temperature is expected since the diffusion activation energy E_d is lower than E_{σ} , Fig. 5b. In other words, the electronic conductivity increases faster with increasing temperature than the ionic transport, resulting in a t_{Ag^+} decrease, $\partial t_{\text{Ag}^+} / \partial T < 0$. In addition, we have observed earlier that the mixed conducting silver selenide and silver telluride glasses are characterized by higher values of the activation energy and pre-exponential factor related to electronic or hole transport.^{19,21,22} In ion-conducting $(\text{CdSe})_x(\text{AgI})_{0.5-x/2}(\text{As}_2\text{Se}_3)_{0.5-x/2}$ glasses, the Haven ratio increases with x from $H_R = 0.4$ to 0.7.¹⁹ Assuming similar trend for the ternary telluride system, we have calculated the silver ion transport numbers. The room temperature t_{Ag^+} values, shown in Figure 7, decrease exponentially with x from 0.67 ± 0.15 ($x = 0$) to $(6.6 \pm 1.8) \times 10^{-4}$ ($x = 0.15$), i.e., by 3 orders of magnitude. The calculated t_{Ag^+} was used to divide the total conductivity σ_{dc} into ionic σ_{Ag^+} and electronic σ_e parts, Figure 8.

The binary $x = 0$ glassy host, $(\text{AgI})_{0.5}(\text{As}_2\text{Te}_3)_{0.5}$, is a mixed conductor with a significant contribution of the Ag^+ ion conductivity, $t_{\text{Ag}^+} = 0.67 \pm 0.15$. Semiconducting CdTe additions induce two opposite processes: (1) a remarkable exponential decrease of the ion transport by a factor of ≈ 200 ; and (2) a monotonic increase of the electronic conductivity by ≈ 1.5 orders of magnitude. The crossover between the two regimes is reflected by a non-monotonic change in σ_{dc} . The electronic conductivity increase with x is caused by Te 5p lone-pair electronic states in the top of the valence band.²³

3.4 Suppression of the Ion Transport

1
2
3
4 We have already reported similar decrease of the ionic conductivity σ_i and ^{110m}Ag tracer
5 diffusion D_{Ag} with increasing x in the ternary selenide system $(\text{CdSe})_x(\text{AgI})_{0.5-}$
6 $x/2(\text{As}_2\text{Se}_3)_{0.5-x/2}$.^{18,19} Comparing the ion transport parameters with those for the binary
7 superionic AgI-As₂Se₃ glasses, it was found that the ternary glasses with the same silver
8 concentration exhibit much lower σ_i and D_{Ag} . A comparable effect is observed for the
9 binary AgI-As₂Te₃ and ternary CdTe-AgI-As₂Te₃ glasses, Figure 9. The diffusion
10 coefficient at 25 °C, D_{298} , for the ternary CdTe-rich glass ($x = 0.15$) appears to be lower
11 by ≈ 2 orders of magnitude in comparison with its binary counterpart, Fig. 9a. The
12 respective diffusion activation energy is higher by 0.2 eV, Fig. 9b.

13
14
15
16 The remarkable suppression of the Ag⁺ ion transport with increasing CdTe content can
17 also have chemical and structural origin similar to that in the selenide system.^{18,19} The
18 exchange reaction $\text{CdTe} + 2\text{AgI} \rightleftharpoons \text{CdI}_2 + \text{Ag}_2\text{Te}$ in the glass-forming melt may lead to a
19 mixed silver environment. As a result, the Ag⁺ ion mobility within the mixed
20 iodide/telluride conduction pathways decreases. Nevertheless, the quantitative analysis
21 of the chemical effect does not reproduce the observed ion transport changes in the
22 ternary selenide glasses.¹⁸ At $x < 0.2$, a significant difference still exists between the
23 simulated and experimental conductivity. A non-random mixing of cadmium and silver
24 species in the ternary glass network appears to be the basis of an additional and/or
25 alternative structural interpretation. Cd-related structural units do not form separate
26 domains but are positioning within the preferential conduction pathways built-up by
27 Ag-related polyhedra. Immobile or slow Cd²⁺ ions will affect the Ag⁺ ion dynamics by
28 restricting the number of accessible empty sites thus reducing the ionic conductivity.
29 The observed increase of the Haven ratio in the selenide system with increasing x is
30 consistent with the non-random mixing but implies immobilisation of some neighboring
31 Ag⁺ cations by a Cd²⁺ ion.¹⁹ Both chemical and structural reasons of the Ag⁺ ion
32 transport suppression need further experimental verification in the ternary telluride
33 system. The experimental conductivity and diffusion data alone do not allow any reliable
34 evidence in favor of either hypothesis to be provided. High-energy x-ray diffraction
35 results could provide a clue for solving the problem.

3.5 Transport Properties in the Telluride and Selenide Ternary Systems

36
37
38
39
40
41
42
43
44
45
46 The two ternary $(\text{CdX})_x(\text{AgI})_{0.5-x/2}(\text{As}_2\text{X}_3)_{0.5-x/2}$ systems, where X = Se or Te, exhibit many
47 similarities and characteristic differences in transport properties, Figure 10. First, the
48 telluride glasses, as the vast majority of vitreous tellurides^{23,24}, have a significantly
49 higher electronic conductivity compared to their selenide counterparts, ≈ 2 orders of
50 magnitude at 25 °C, Fig. 10a. The observed difference is caused by Te 5p lone-pair
51 electron states forming the top of the valence band in telluride alloys compared to lower
52 lying Se 4p lone pairs.^{23,25}

1
2
3 On the contrary, the ionic conductivity and silver tracer diffusion coefficient are by a
4 factor of 100 to 300 higher in the selenide ternaries, Fig. 10b, accompanied also by lower
5 activation energy. Similar decrease of D_{Ag} was reported earlier for mixed chalcogen Ag-
6 As-Se-Te glasses²¹, when Se was progressively replaced by Te. Only the intermediate
7 compositions with Te fraction $r = \text{Te}/(\text{Se}+\text{Te})$ in the range of $0.05 \leq r \leq 0.35$, have shown
8 a non-monotonic change in D_{Ag} , attributed to a mixed anion effect. The reason of the
9 observed difference in the magnitude of σ_i and D_{Ag} between telluride and selenide
10 systems is not yet clear. Detailed structural studies are needed to compare the
11 connectivity of Ag-related sub-network in the two families. Finally, the effect of CdX (X =
12 Se or Te) additions is identical for the two systems. Semiconducting cadmium
13 chalcogenides increase the electronic conductivity and decrease the ionic one. Even
14 quantitatively, the observed changes are similar: D_{Ag} decreases of 2-2.5 orders of
15 magnitude and σ_e increases by a factor of 10-30.
16
17
18
19
20
21

22 4. CONCLUSIONS

23
24 The ^{110m}Ag tracer diffusion coefficient in the $(\text{CdTe})_x(\text{AgI})_{0.5-x/2}(\text{As}_2\text{Te}_3)_{0.5-x/2}$ glasses (0.0
25 $\leq x \leq 0.15$) decreases by a factor of ≈ 200 with increasing x from $6.8 \times 10^{-11} \text{ cm}^2 \text{ s}^{-1}$ ($x =$
26 0.0) to $3.8 \times 10^{-13} \text{ cm}^2 \text{ s}^{-1}$ ($x = 0.15$) at room temperature. The D_{Ag} decrease is
27 accompanied by a simultaneous increase of the diffusion activation energy from 0.47 eV
28 to 0.68 eV and the diffusion pre-exponential factor by a factor of 15. The combined
29 analysis of diffusion and conductivity data shows a significant decrease of the silver ion
30 transport number by three orders of magnitude with increasing x . The suppression of
31 the Ag^+ ion transport accompanied by a simultaneous increase of the electronic
32 conductivity causes an ionic-to-electronic transport crossover in cadmium telluride
33 glasses; the CdTe-rich vitreous alloys become nearly pure electronic conductors.
34
35
36
37
38

39 AUTHOR INFORMATION

40 41 **Corresponding Author**

42 *E-mail: Mohamad.Kassem@univ-littoral.fr. Phone: +33-328-658270.

43 **Author Contributions**

44 The manuscript was written through contributions of all authors. All authors have given
45 approval to the final version of the manuscript.

46 **Notes**

47 The authors declare no competing financial interest.
48
49
50

51 ACKNOWLEDGMENTS

52
53 This work was supported by the European Commission within the Interreg IIIA (CTMM
54 project) and Interreg IVA (CleanTech project) programmes and by Agence Nationale de
55 la Recherche (ANR, France) under Grant No. ANR-15-ASTR-0016-01.
56
57
58
59
60

RERERENCES

- (1) Terai, R.; Hayami, R. Ionic Diffusion in Glasses. *J. Non-Cryst. Solids* **1975**, *18*, 217–264.
- (2) Frischat, G.H. Ionic Diffusion in Oxide Glasses. *Trans Tech Publications* **1975**.
- (3) Natrup, F.V.; Bracht, H.; Murugavel, S.; Roling, B. Cation Diffusion and Ionic Conductivity in Soda-Lime Silicate Glasses. *Phys. Chem. Chem. Phys.* **2005**, *7*, 2279–2286.
- (4) Mehrer, H.; Imre, A. W.; Tanguiep-Nijokep, E. Diffusion and Ionic Conduction in Oxide Glasses. *J. Phys. Conf. Series* **2008**, *106*, 012001
- (5) Kawamoto, Y.; Nishida, M. Silver Diffusion in $\text{As}_2\text{S}_3\text{-Ag}_2\text{S}$, $\text{GeS}_2\text{-GeS-Ag}_2\text{S}$ and $\text{P}_2\text{S}_5\text{-Ag}_2\text{S}$ Glasses. *Phys. Chem. Glasses* **1977**, *18*, 19–23.
- (6) Kazakova, E.A. A Study of Silver-Containing Chalcogenide Glasses. Leningrad University: Ph.D. Thesis. Leningrad, **1980**.
- (7) Thomas, M.P.; Peterson, N.L.; Hutchinson, E. Tracer Diffusion and Electrical Conductivity in Sodium-Rubidium Silicon Sulfide Glasses. *J. Am. Ceram. Soc.* **1985**, *68*, 99–104.
- (8) Bychkov, E.; Tsegelnik, V.; Vlasov, Yu.; Pradel, A.; Ribes, M. Percolation Transition in Ag-Doped Germanium Chalcogenide-Based Glasses: Conductivity and Silver Diffusion Results. *J. Non-Cryst. Solids* **1996**, *208*, 1–20.
- (9) Bychkov, E.; Bychkov, A.; Pradel, A.; Ribes, M. Percolation Transition in Ag-Doped Chalcogenide Glasses: Comparison of Classical Percolation and Dynamic Structure Models. *Solid State Ionics* **1998**, *113–115*, 691–695.
- (10) Drugov, Yu.; Tsegelnik, V.; Bolotov, A.; Vlasov, Yu.; Bychkov, E. ^{110}Ag Tracer Diffusion Study of Percolation Transition in $\text{Ag}_2\text{S-As}_2\text{S}_3$ Glasses. *Solid State Ionics* **2000**, *136–137*, 1091–1096.
- (11) Bychkov, E.; Bolotov, A.; Tsegelnik, V.; Grushko, Yu.; Vlasov, Yu. ^{64}Cu Tracer Diffusion in Copper Chalcogenide Glasses. *Defect Diffus. Forum* **2001**, *194–199*, 919–924.
- (12) Bychkov, E.; Bolotov, A.; Grushko, Y.S.; Vlasov, Yu.; Wortmann, G. Ionic Diffusion and Local Hopping in Copper Chalcohalide Glasses Measured Using ^{64}Cu Tracer and ^{129}I -Mössbauer Spectroscopy. *Solid State Ionics* **1996**, *90*, 289–294.
- (13) Bychkov, E.; Bolotov, A.; Armand, P.; Ibanez, A. EXAFS Studies of Cu^+ Ion Conducting and Semiconducting Copper Chalcogenide and Chalcohalide Glasses. *J. Non-Cryst. Solids* **1998**, *232–234*, 314–322.

- 1
2
3 (14) Bolotov, A.; Bychkov, E.; Gavrilov, Yu.; Grushko, Yu.; Pradel, A.; Ribes, M.;
4 Tsegelnik, V.; Vlasov, Yu. Degenerated Mixed Cation Effect in CuI–AgI–As₂Se₃
5 Glasses: ⁶⁴Cu and ¹¹⁰Ag Tracer Diffusion Studies. *Solid State Ionics* **1998**, *113–115*,
6 697–701.
7
8 (15) Kassem, M.; Le Coq, D.; Boidin, R.; Bychkov, E. New Chalcogenide Glasses in the
9 CdTe–AgI–As₂Te₃ System. *Materials Research Bulletin* **2012**, *47*, 193–198.
10
11 (16) Bobylev, Yu.V.; Bychkov, E.A.; Tver'yanovich, Yu.S. Electrical Properties of Glasses
12 in the AgI–As₂Te₃ System. *Glass Physics and Chemistry* **2004**, *30*, 519–522.
13
14 (17) Alekseev, I.; Kassem, M.; Fourmentin, M.; Le Coq, D.; Iizawa, R.; Usuki, T.; Bychkov,
15 E. Ionic and Electronic Transport in AgI–As₂Te₃ Glasses. *Solid State Ionics* **2013**,
16 *253*, 181–184.
17
18 (18) Kassem, M.; Le Coq, D.; Bokova, M.; Bychkov, E. Chemical and Structural Origin of
19 Conductivity Changes in CdSe–AgI–As₂Se₃ Glasses. *Solid State Ionics* **2010**, *181*,
20 466–472.
21
22 (19) Alekseev, I.; Kassem, M.; Le Coq, D.; Bokova, M.; Fourmentin, M.; Bychkov, E. ¹¹⁰Ag
23 Tracer Diffusion Studies of CdSe–AgI–As₂Se₃ Glasses. *Solid State Ionics* **2010**, *181*,
24 1467–1472.
25
26 (20) Murch, G.E. The Haven Ratio in Fast Ionic Conductors. *Solid State Ionics* **1982**, *7*,
27 177–198.
28
29 (21) Vlasov, Yu.G.; Bychkov, E.A.; Seleznev, B.L. Compositional Dependence of Ionic
30 Conductivity and Diffusion in Mixed Chalcogen Ag-Containing Glasses. *Solid State*
31 *Ionics* **1987**, *24*, 179–187.
32
33 (22) Vlasov, Yu.G.; Bychkov, E.A. Ionic and Electronic Conductivity in the Copper-
34 Silver-Arsenic-Selenium Glasses. *Solid State Ionics* **1984**, *14*, 329–335.
35
36 (23) Mott, N.F.; Davis, E.A. *Electronic Processes in Non-Crystalline Materials*.
37 Clarendon Press, Oxford, **1979**.
38
39 (24) Adam J.-L.; Zhang, X. (Editors) *Chalcogenide Glasses: Preparation, properties and*
40 *applications*. Woodhead Publishing, Oxford – Cambridge – Philadelphia – New
41 Delhi, **2014**.
42
43 (25) Kolobov, A. V.; Tominaga, J. *Chalcogenides. Metastability and Phase Change*
44 *Phenomena*. Springer, Heidelberg – New York – Dordrecht – London, **2012**.
45
46
47
48
49
50
51
52
53
54
55
56
57
58
59
60

List of Figures

1. Typical ^{110m}Ag tracer diffusion profile for a $(\text{CdTe})_{0.05}(\text{AgI})_{0.475}(\text{As}_2\text{Te}_3)_{0.475}$ glass annealed at 45 °C for 17 days. The filled circles correspond to penetration depth calculated using weight changes; the open symbols represent direct thickness measurements. The solid line shows a least-square fit of the experimental data points to Equation (2) where $q = \text{erf}^{-1}\left(1 - \frac{A(y, t)}{A_0}\right)$.
2. Temperature dependences of the silver tracer diffusion coefficient for glasses in the ternary system $(\text{CdTe})_x(\text{AgI})_{0.5-x/2}(\text{As}_2\text{Te}_3)_{0.5-x/2}$. The solid lines represent a least-square fit of the data to Equation (3).
3. Composition dependences of both (●) diffusion and (●) conductivity parameters for the ternary $(\text{CdTe})_x(\text{AgI})_{0.5-x/2}(\text{As}_2\text{Te}_3)_{0.5-x/2}$ glasses: (a) room-temperature silver tracer diffusion coefficient D_{Ag} and conductivity diffusion coefficient D_{σ} calculated using the Nernst-Einstein relation; (b) diffusion activation energy E_d ; (c) diffusion pre-exponential factor D_0 . All solid lines are drawn as a guide to the eye.
4. Apparent Haven ratio $t_{\text{Ag}^+}H_{\text{R}}$ for the CdTe-AgI-As₂Te₃ glasses plotted as a function of temperature.
5. Total conductivity σ_{dc} and ionic transport parameters for the ternary CdTe-AgI-As₂Te₃ glasses: (a) room-temperature σ_{dc} and $H_{\text{R}}\sigma_{\text{Ag}^+}$; (b) the conductivity E_{σ} and diffusion E_d activation energies, and (c) the conductivity σ_0 and recalculated diffusion $H_{\text{R}}\sigma_0(\text{Ag}^+)$ pre-exponential factors. All solid lines are a guide to the eye.
6. Silver ion transport number t_{Ag^+} plotted as a function of temperature for selected $(\text{CdTe})_x(\text{AgI})_{0.5-x/2}(\text{As}_2\text{Te}_3)_{0.5-x/2}$ glasses, $x = 0$ and 0.05.
7. Room temperature silver ion transport number t_{Ag^+} for the ternary $(\text{CdTe})_x(\text{AgI})_{0.5-x/2}(\text{As}_2\text{Te}_3)_{0.5-x/2}$ glasses plotted as a function of CdTe content.

- 1
- 2
- 3 8. Room temperature total conductivity σ_{dc} as well as its ionic σ_{Ag^+} and electronic σ_e
- 4 components for the ternary CdTe-AgI-As₂Te₃ glasses.
- 5
- 6
- 7 9. (a) Room temperature diffusion coefficient D_{Ag} , and (b) diffusion activation
- 8 energy E_d for the binary AgI-As₂Te₃¹⁷ and ternary CdTe-AgI-As₂Te₃ glasses
- 9 plotted as a function of the silver content. The solid lines are drawn as a guide to
- 10 the eye.
- 11
- 12
- 13
- 14
- 15 10. Room-temperature transport characteristics of the ternary (CdX)_x(AgI)_{0.5-}
- 16 _{$x/2$} (As₂X₃)_{0.5-x/2} glasses, where X = Se or Te: (a) electronic conductivity; (b) ^{110m}Ag
- 17 tracer diffusion coefficient.
- 18
- 19
- 20
- 21
- 22
- 23
- 24
- 25
- 26
- 27
- 28
- 29
- 30
- 31
- 32
- 33
- 34
- 35
- 36
- 37
- 38
- 39
- 40
- 41
- 42
- 43
- 44
- 45
- 46
- 47
- 48
- 49
- 50
- 51
- 52
- 53
- 54
- 55
- 56
- 57
- 58
- 59
- 60

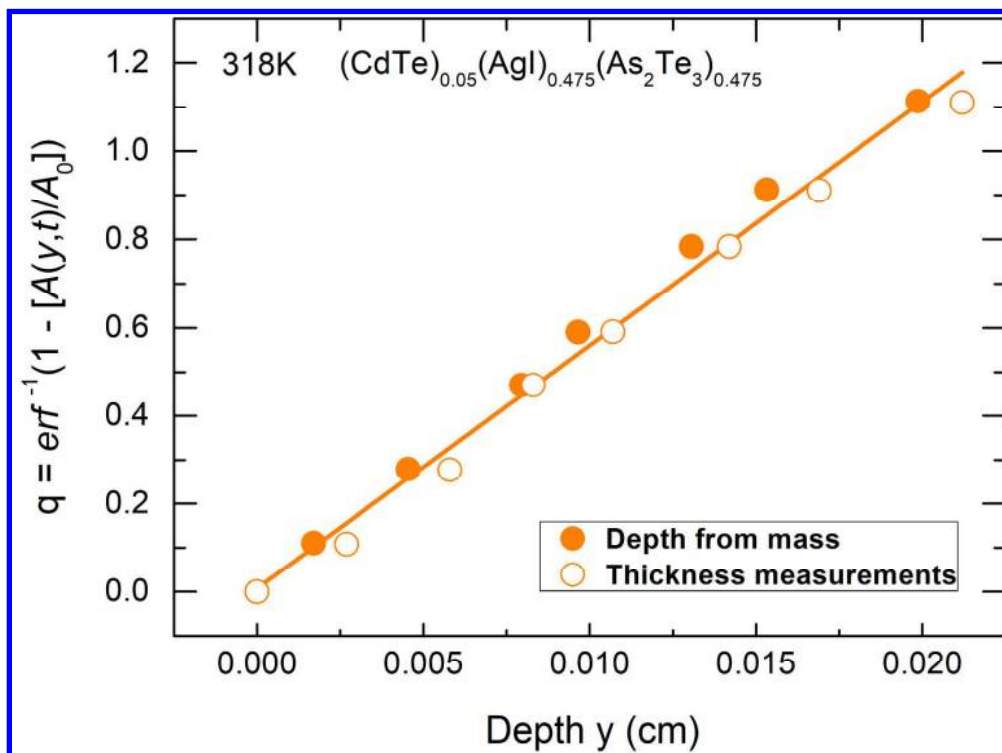


Fig. 1. Typical $^{110\text{m}}\text{Ag}$ tracer diffusion profile for a $(\text{CdTe})_{0.05}(\text{AgI})_{0.475}(\text{As}_2\text{Te}_3)_{0.475}$ glass annealed at 45°C for 17 days. The penetration depth was calculated using (a) weight changes (filled circles) and (b) direct thickness measurements (open circles). The solid line shows a least-square fit of all experimental data points (open and filled circles) to

Equation (2) where $q = \text{erf}^{-1}\left(1 - \frac{A(y,t)}{A_0}\right)$.

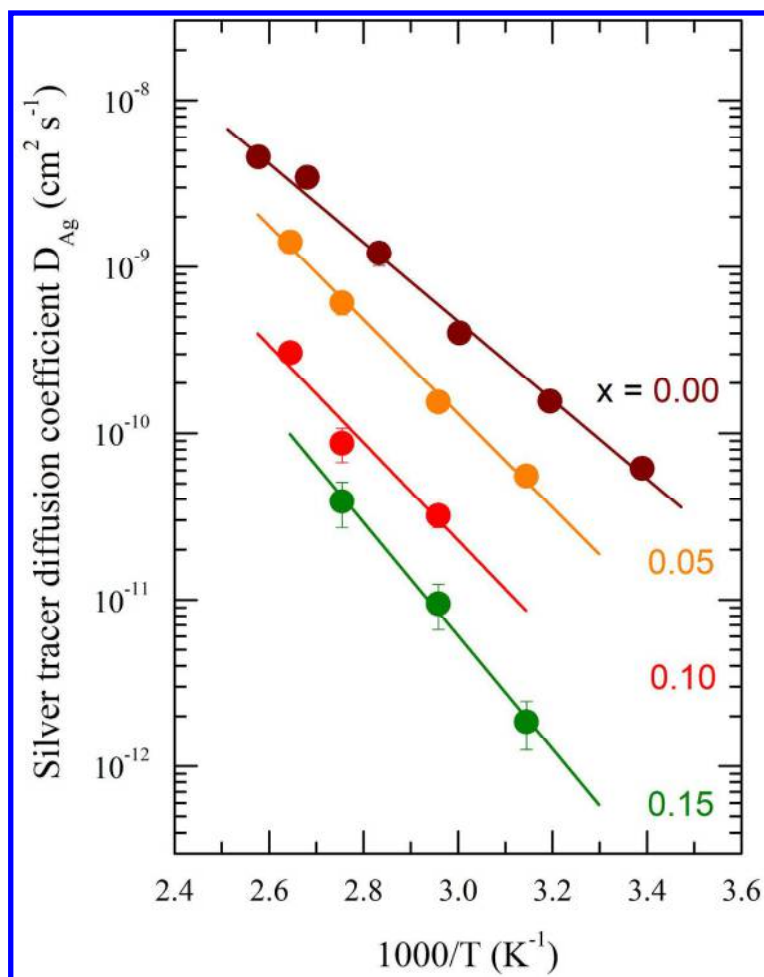


Fig. 2. Temperature dependences of the silver tracer diffusion coefficient for glasses in the ternary system $(\text{CdTe})_x(\text{AgI})_{0.5-x/2}(\text{As}_2\text{Te}_3)_{0.5-x/2}$. The solid lines represent a least-square fit of the data to Equation (3).

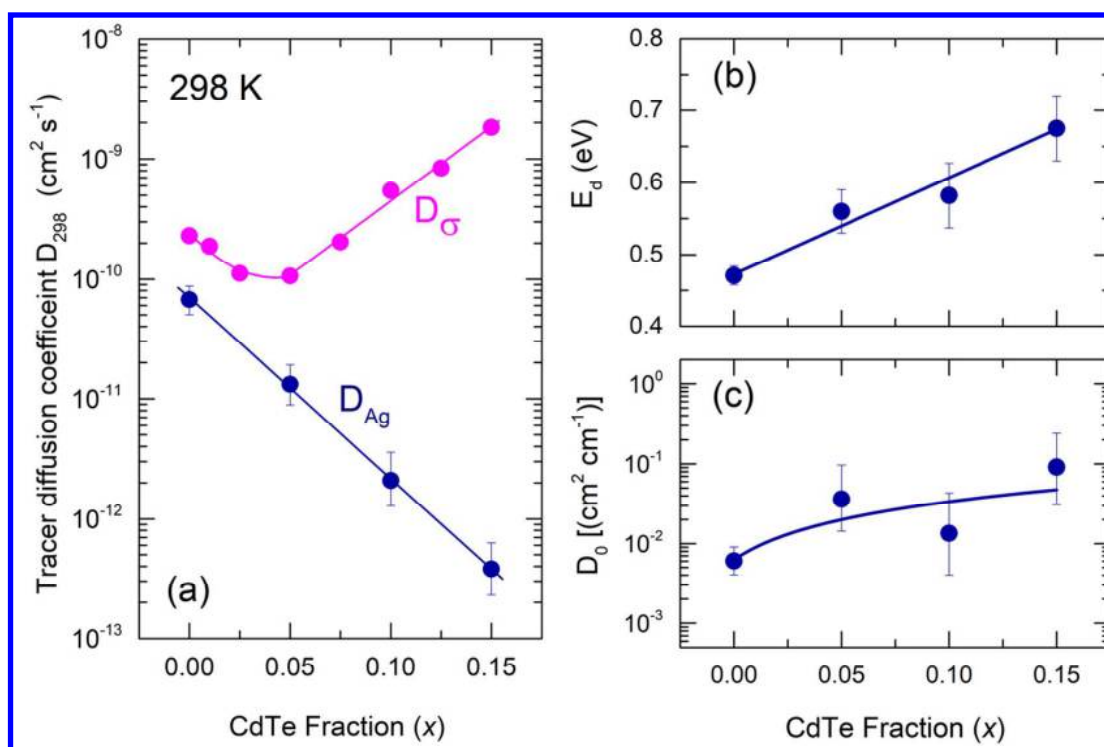


Fig. 3. Composition dependences of both (●) diffusion and (●) conductivity parameters for the ternary $(\text{CdTe})_x(\text{AgI})_{0.5-x/2}(\text{As}_2\text{Te}_3)_{0.5-x/2}$ glasses: (a) room-temperature silver tracer diffusion coefficient D_{Ag} and conductivity diffusion coefficient calculated using the Nernst-Einstein relation; (b) diffusion activation energy E_d ; (c) diffusion pre-exponential factor D_0 . All solid lines are drawn as a guide to the eye.

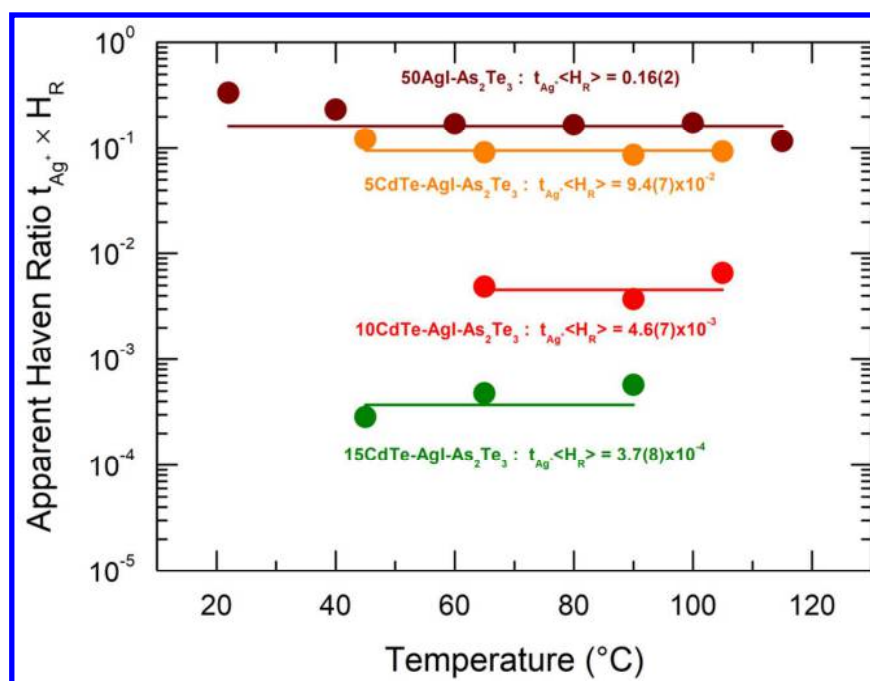


Fig. 4. Apparent Haven ratio $t_{Ag^+}H_R$ for the CdTe-AgI-As₂Te₃ glasses plotted as a function of temperature.

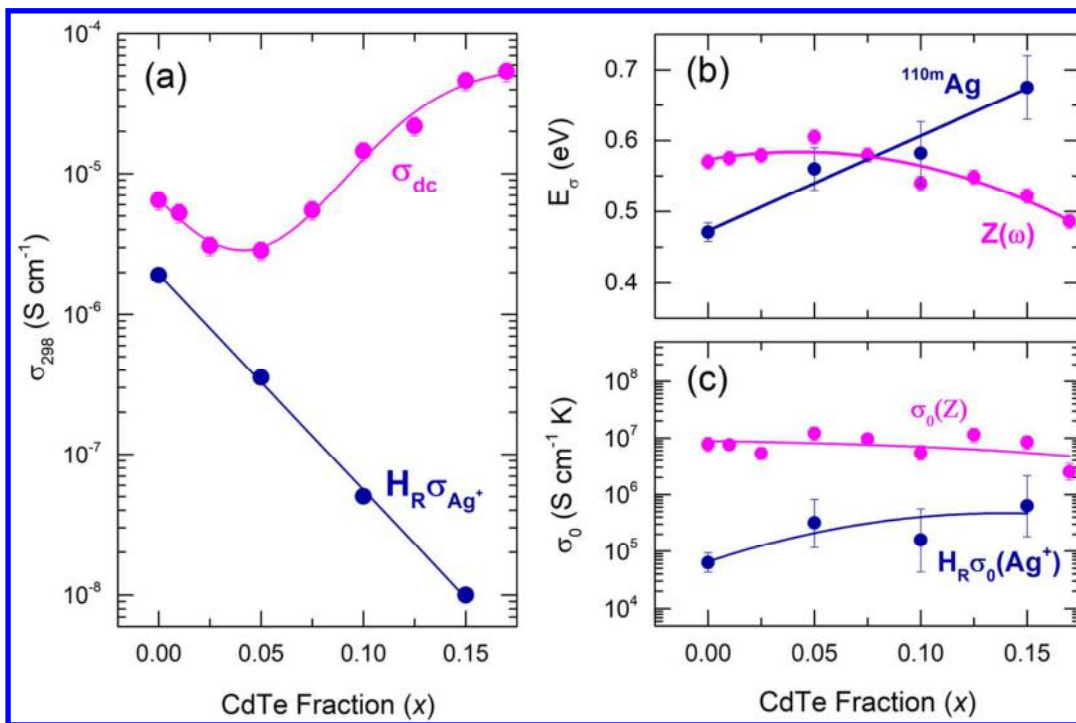


Fig. 5. Total conductivity σ_{dc} and ionic transport parameters for the ternary CdTe-AgI-As₂Te₃ glasses: (a) room-temperature σ_{dc} and $H_R \sigma_{Ag^+}$; (b) the conductivity E_σ and diffusion E_d activation energies, and (c) the conductivity σ_0 and recalculated diffusion $H_R \sigma_0(Ag^+)$ pre-exponential factors. All solid lines are a guide to the eye.

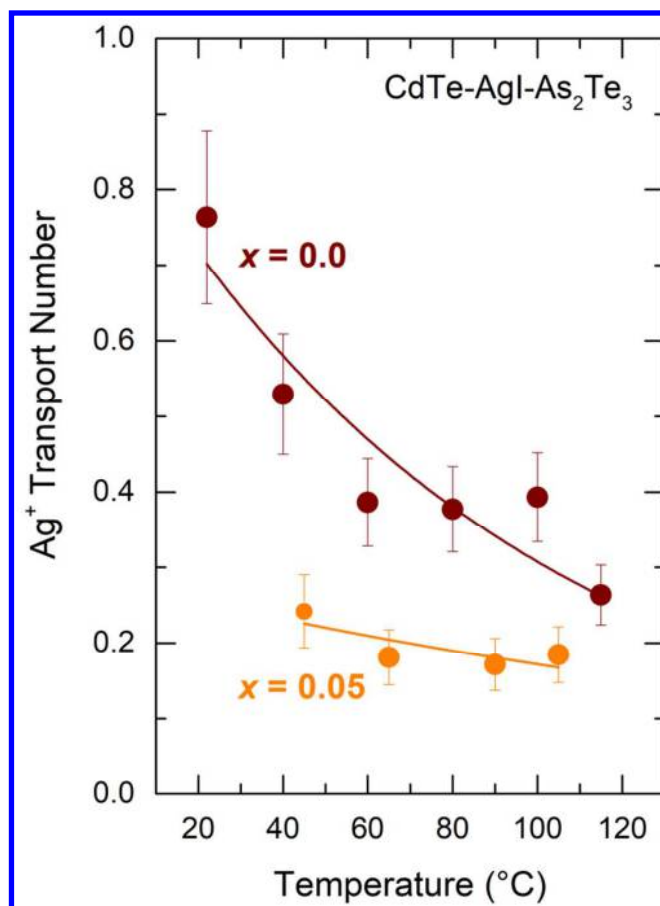


Fig. 6. Silver ion transport number t_{Ag^+} plotted as a function of temperature for selected $(CdTe)_x(AgI)_{0.5-x/2}(As_2Te_3)_{0.5-x/2}$ glasses, $x = 0$ and 0.05 .

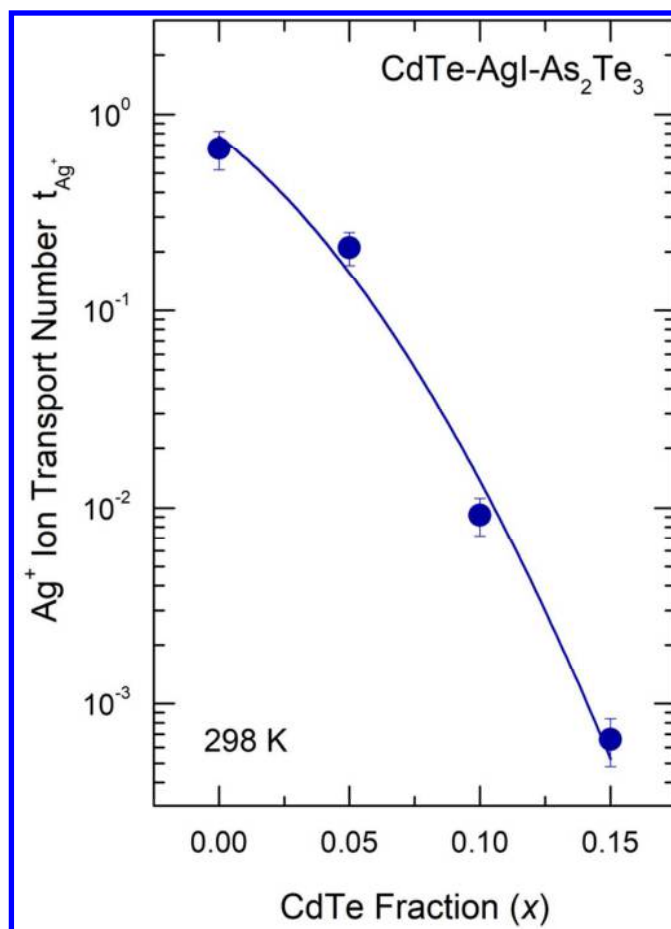


Fig. 7. Room temperature silver ion transport number t_{Ag^+} for the ternary $(CdTe)_x(AgI)_{0.5-x/2}(As_2Te_3)_{0.5-x/2}$ glasses plotted as a function of CdTe content.

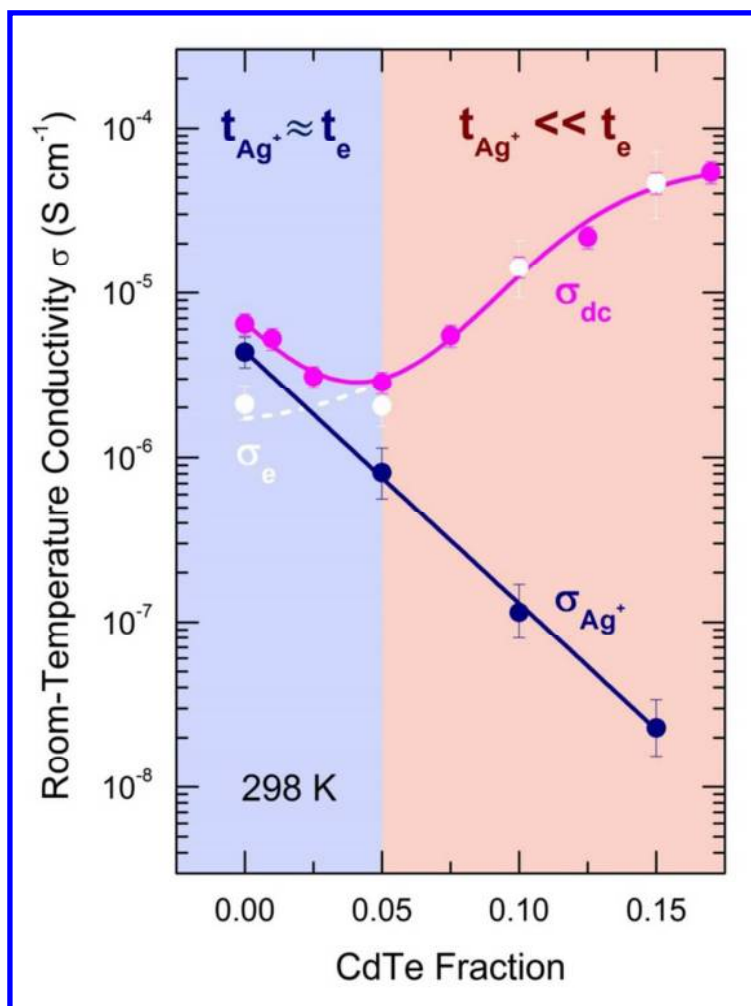


Fig. 8. Room temperature total conductivity σ_{dc} as well as its ionic σ_{Ag^+} and electronic σ_e components for the ternary CdTe-AgI-As₂Te₃ glasses.

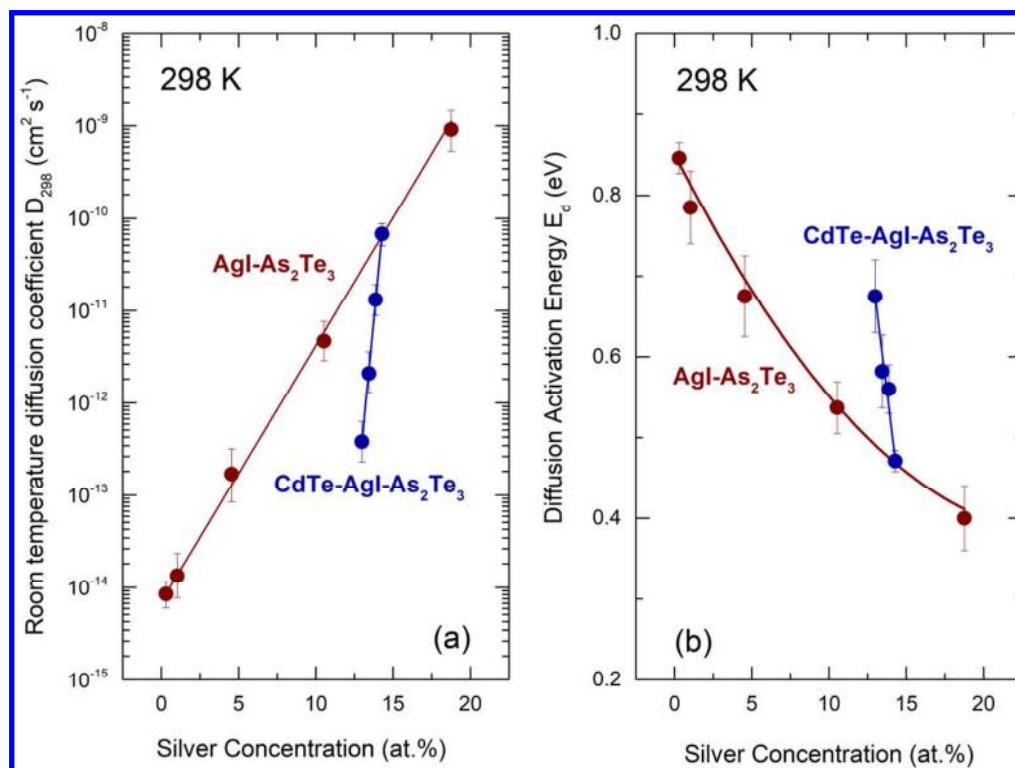


Fig. 9. (a) Room temperature diffusion coefficient D_{Ag} , and (b) diffusion activation energy E_d for the binary AgI-As₂Te₃¹⁷ and ternary CdTe-AgI-As₂Te₃ glasses plotted as a function of the silver content. The solid lines are drawn as a guide to the eye.

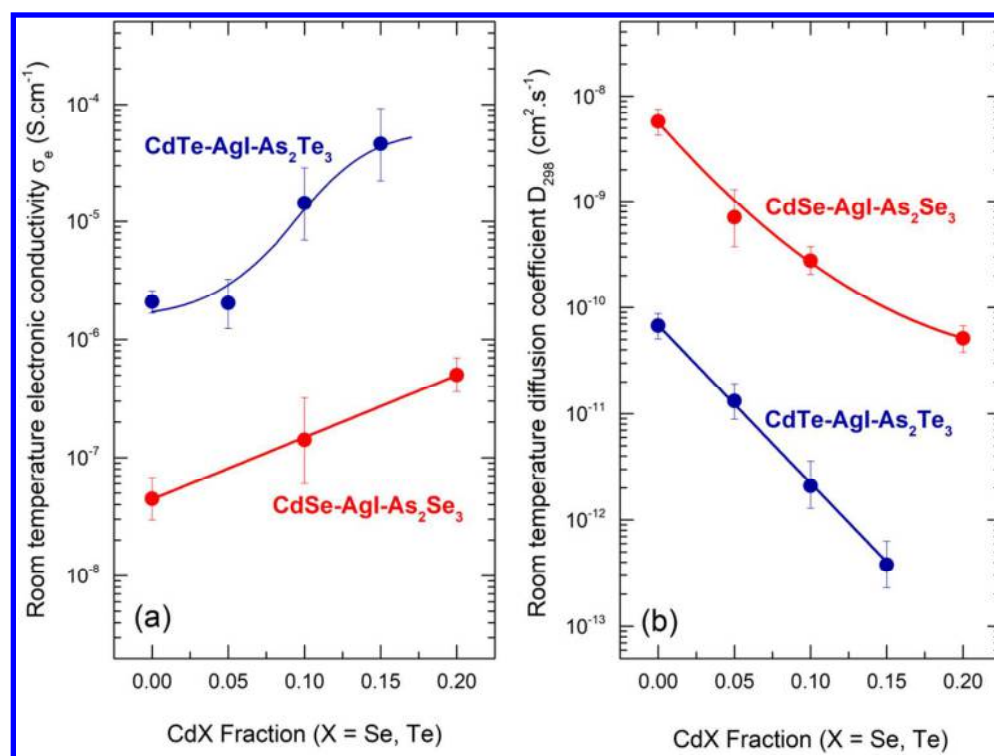


Fig. 10. Room-temperature transport characteristics of the ternary $(\text{CdX})_x(\text{AgI})_{0.5-x/2}(\text{As}_2\text{X}_3)_{0.5-x/2}$ glasses, where $X = \text{Se}$ or Te : (a) electronic conductivity; (b) $^{110\text{m}}\text{Ag}$ tracer diffusion coefficient.

List of Tables

- ^{110m}Ag tracer diffusion parameters for the CdTe-AgI-As₂Te₃ glasses: the room-diffusion coefficient D_{298} , the diffusion activation energy E_d , the pre-exponential factor D_0 , and the apparent Haven ratio $t_{\text{Ag}^+}H_R$

Table 1

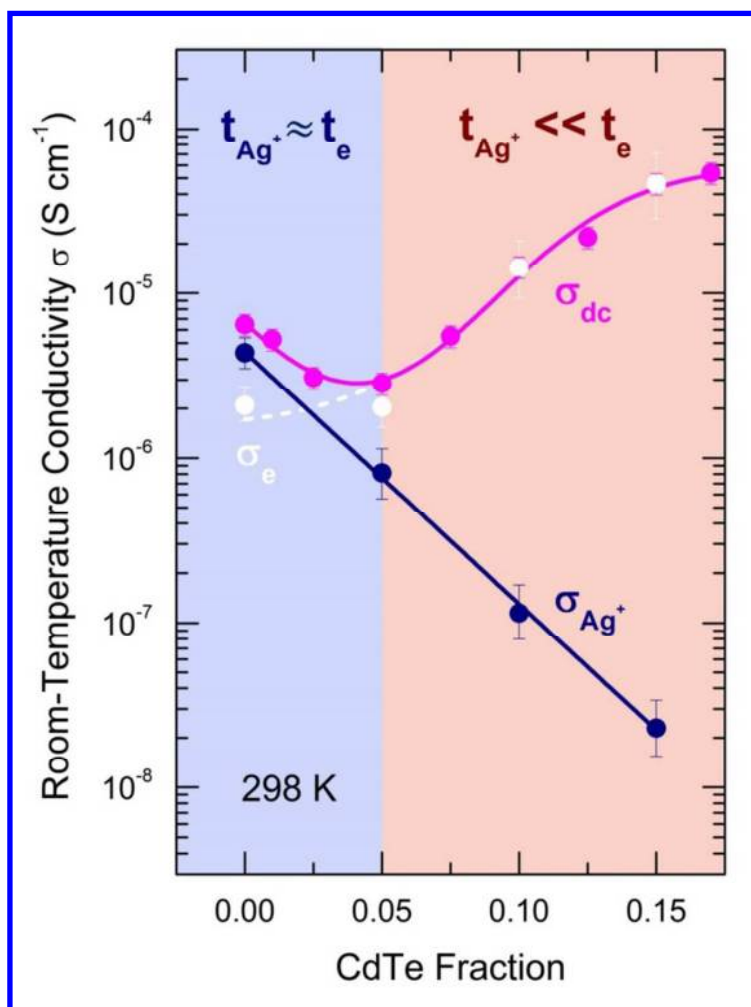
^{110m}Ag tracer diffusion parameters for the CdTe-AgI-As₂Te₃ glasses: the room-diffusion coefficient D_{298} , the diffusion activation energy E_d , the pre-exponential factor D_0 , and the apparent Haven ratio $t_{\text{Ag}^+}H_R$

| Composition | | D_{298} (cm ² s ⁻¹) | E_d (eV) | D_0 (cm ² s ⁻¹) | $t_{\text{Ag}^+}H_R$ |
|---|-------------|--|------------|--|-------------------------|
| $(\text{CdTe})_x(\text{AgI})_{0.5-x/2}(\text{As}_2\text{Te}_3)_{0.5-x/2}$ | | | | | |
| x | [Ag] (at.%) | | | | |
| 0.00 | 14.28 | 6.8×10^{-11} | 0.471(13) | 6.0×10^{-3} | $1.6(2) \times 10^{-1}$ |
| 0.05 | 13.87 | 1.3×10^{-11} | 0.560(31) | 3.6×10^{-2} | $9.4(7) \times 10^{-2}$ |
| 0.10 | 13.43 | 2.1×10^{-12} | 0.582(45) | 1.3×10^{-2} | $4.6(7) \times 10^{-3}$ |
| 0.15 | 12.98 | 3.8×10^{-13} | 0.675(46) | 9.1×10^{-2} | $3.7(8) \times 10^{-4}$ |

Uncertainties in the last digit(s) of the parameter are given in parentheses.

The apparent Haven ratio $t_{\text{Ag}^+}H_R$ averaged over the temperature range of diffusion measurements.

TOC graphic



| Composition | | D_{298} (cm ² s ⁻¹) | E_d (eV) | D_0 (cm ² s ⁻¹) | $t_{Ag^+}H_R$ |
|---|-------------|--|------------|--|-------------------------|
| $(CdTe)_x(AgI)_{0.5-x/2}(As_2Te_3)_{0.5-x/2}$ | | | | | |
| x | [Ag] (at.%) | | | | |
| 0.00 | 14.28 | 6.8×10^{-11} | 0.471(13) | 6.0×10^{-3} | $1.6(2) \times 10^{-1}$ |
| 0.05 | 13.87 | 1.3×10^{-11} | 0.560(31) | 3.6×10^{-2} | $9.4(7) \times 10^{-2}$ |
| 0.10 | 13.43 | 2.1×10^{-12} | 0.582(45) | 1.3×10^{-2} | $4.6(7) \times 10^{-3}$ |
| 0.15 | 12.98 | 3.8×10^{-13} | 0.675(46) | 9.1×10^{-2} | $3.7(8) \times 10^{-4}$ |
| <i>Uncertainties in the last digit(s) of the parameter are given in parentheses.</i> | | | | | |
| <i>The apparent Haven ratio $t_{Ag^+}H_R$ averaged over the temperature range of diffusion measurements.</i> | | | | | |

^{110m}Ag tracer diffusion parameters for the CdTe-AgI-As₂Te₃ glasses: the room-diffusion coefficient D_{298} , the diffusion activation energy E_d , the pre-exponential factor D_0 , and the apparent Haven ratio $t_{Ag^+}H_R$

248x84mm (96 x 96 DPI)

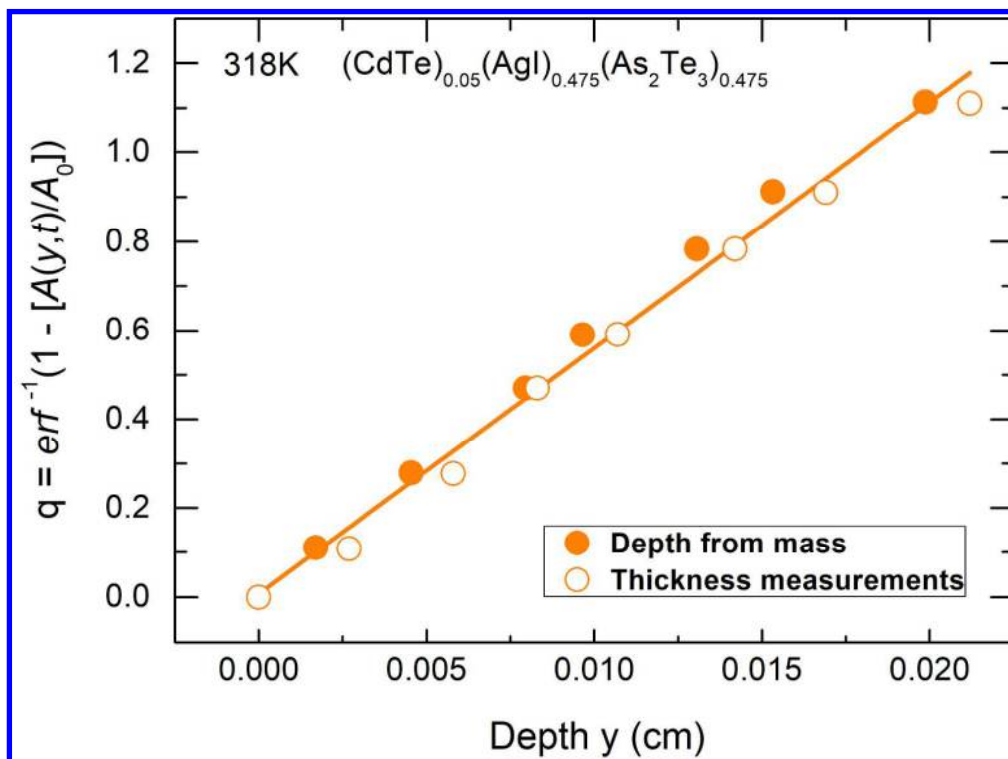


Figure 1. Typical $^{110\text{m}}\text{Ag}$ tracer diffusion profile for a $(\text{CdTe})_{0.05}(\text{AgI})_{0.475}(\text{As}_2\text{Te}_3)_{0.475}$ glass annealed at $45\text{ }^\circ\text{C}$ for 17 days. The penetration depth was calculated using (a) weight changes (filled circles) and (b) direct thickness measurements (open circles). The solid line shows a least-square fit of all experimental data points (open and filled circles) to Equation (2) where $q = \text{erf}^{-1}(1 - A(y,t)/A_0)$.

241x179mm (300 x 300 DPI)

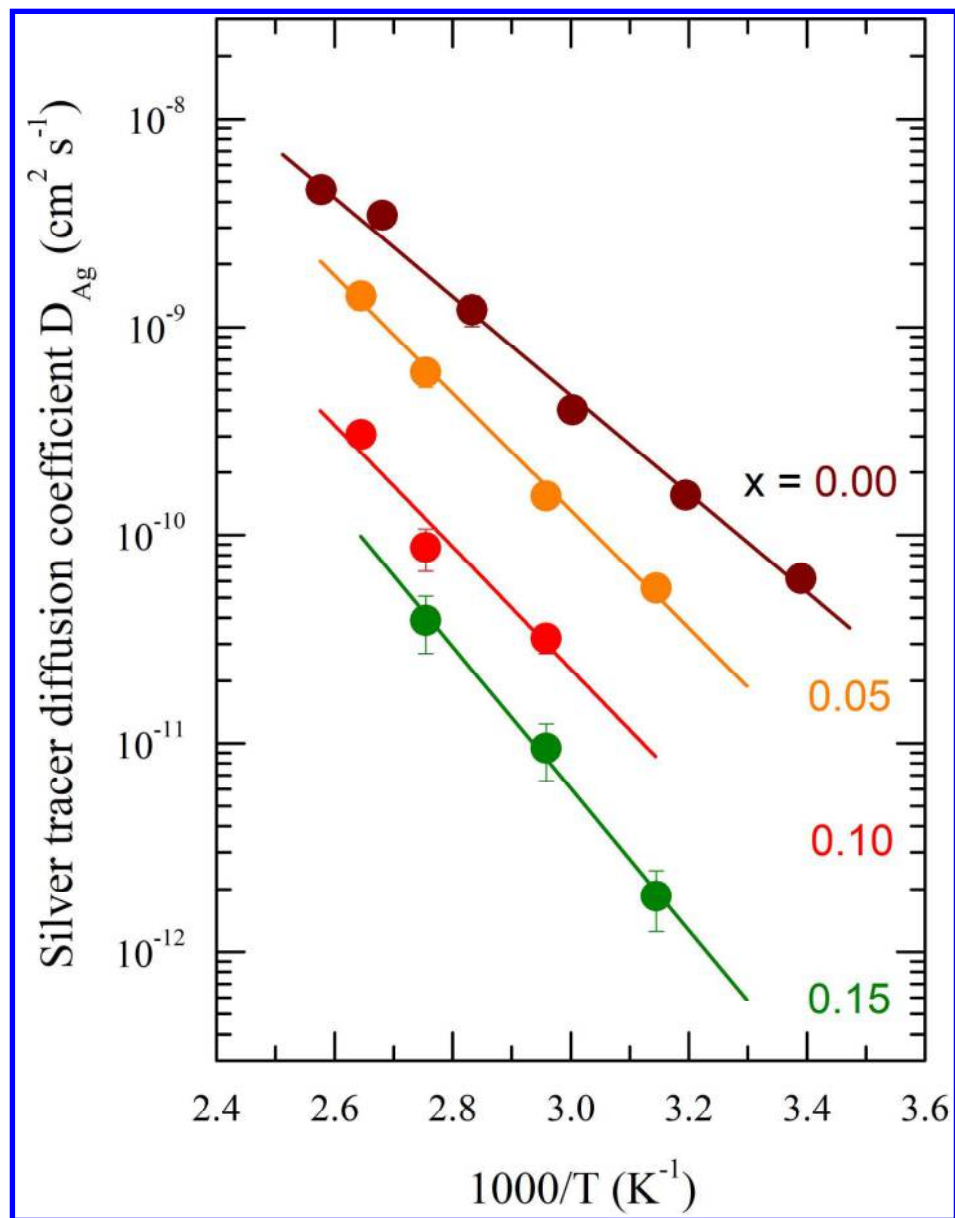


Figure 2. Temperature dependences of the silver tracer diffusion coefficient for glasses in the ternary system $(\text{CdTe})_x(\text{AgI})_{0.5-x/2}(\text{As}_2\text{Te}_3)_{0.5-x/2}$. The solid lines represent a least-square fit of the data to Equation (3).

182x234mm (300 x 300 DPI)

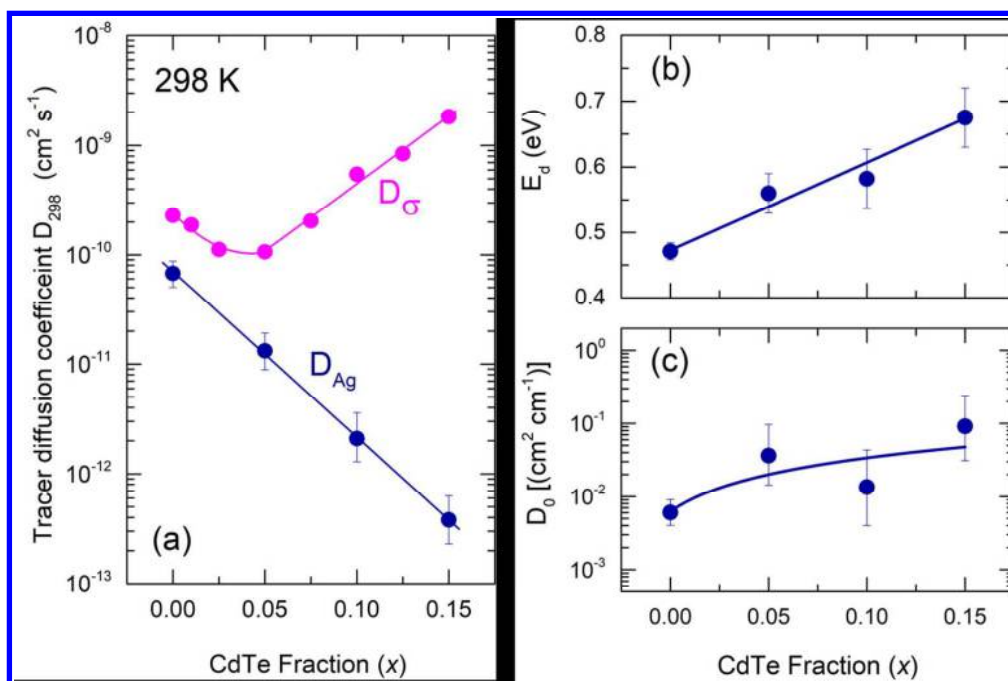


Figure 3. Composition dependences of both (●) diffusion and (●) conductivity parameters for the ternary $(\text{CdTe})_x(\text{AgI})_{0.5-x/2}(\text{As}_2\text{Te}_3)_{0.5-x/2}$ glasses: (a) room-temperature silver tracer diffusion coefficient D_{Ag} and conductivity diffusion coefficient D_{σ} calculated using the Nernst-Einstein relation; (b) diffusion activation energy E_d ; (c) diffusion pre-exponential factor D_0 . All solid lines are drawn as a guide to the eye.

233x154mm (150 x 150 DPI)

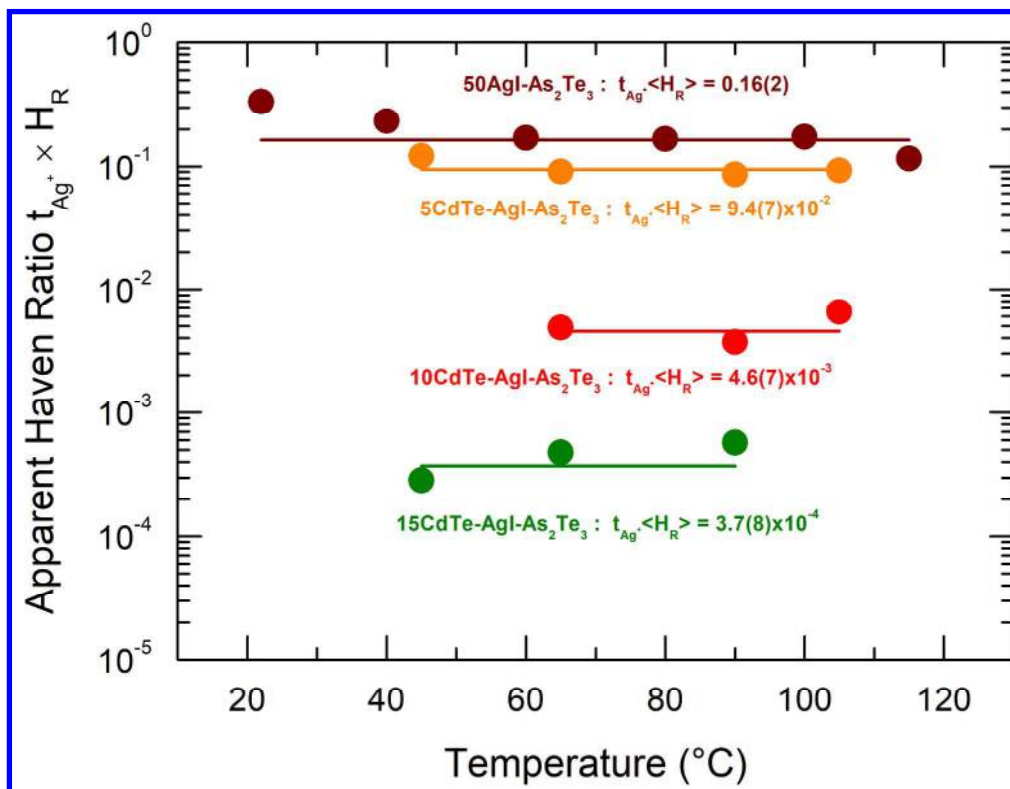


Figure 4. Apparent Haven ratio $t_{Ag^+} H_R$ for the CdTe-AgI-As₂Te₃ glasses plotted as a function of temperature.

234x180mm (300 x 300 DPI)

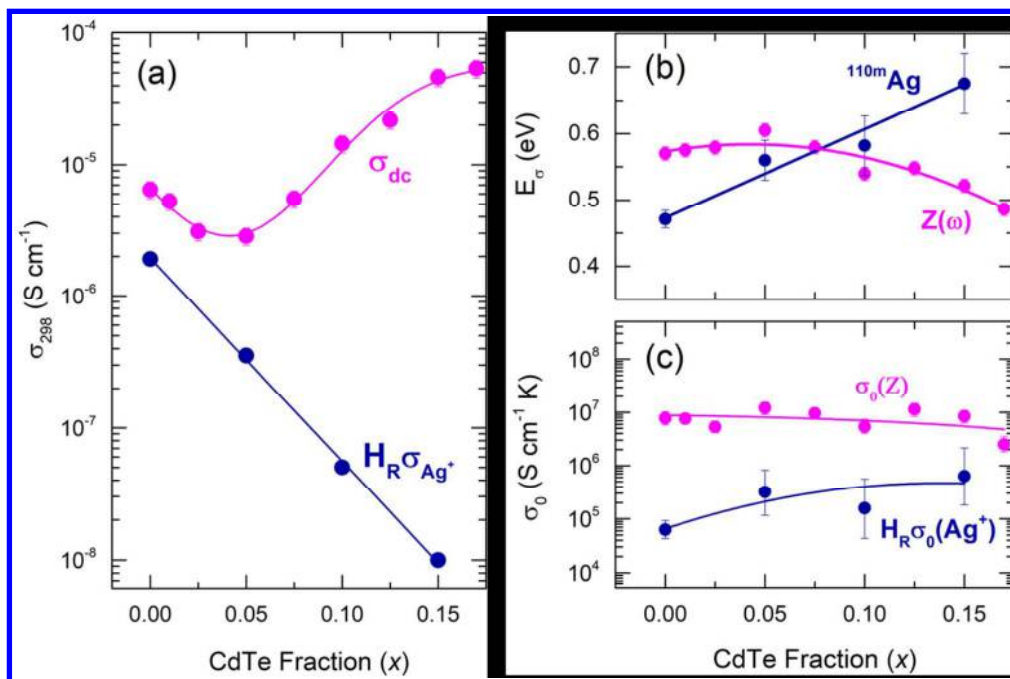
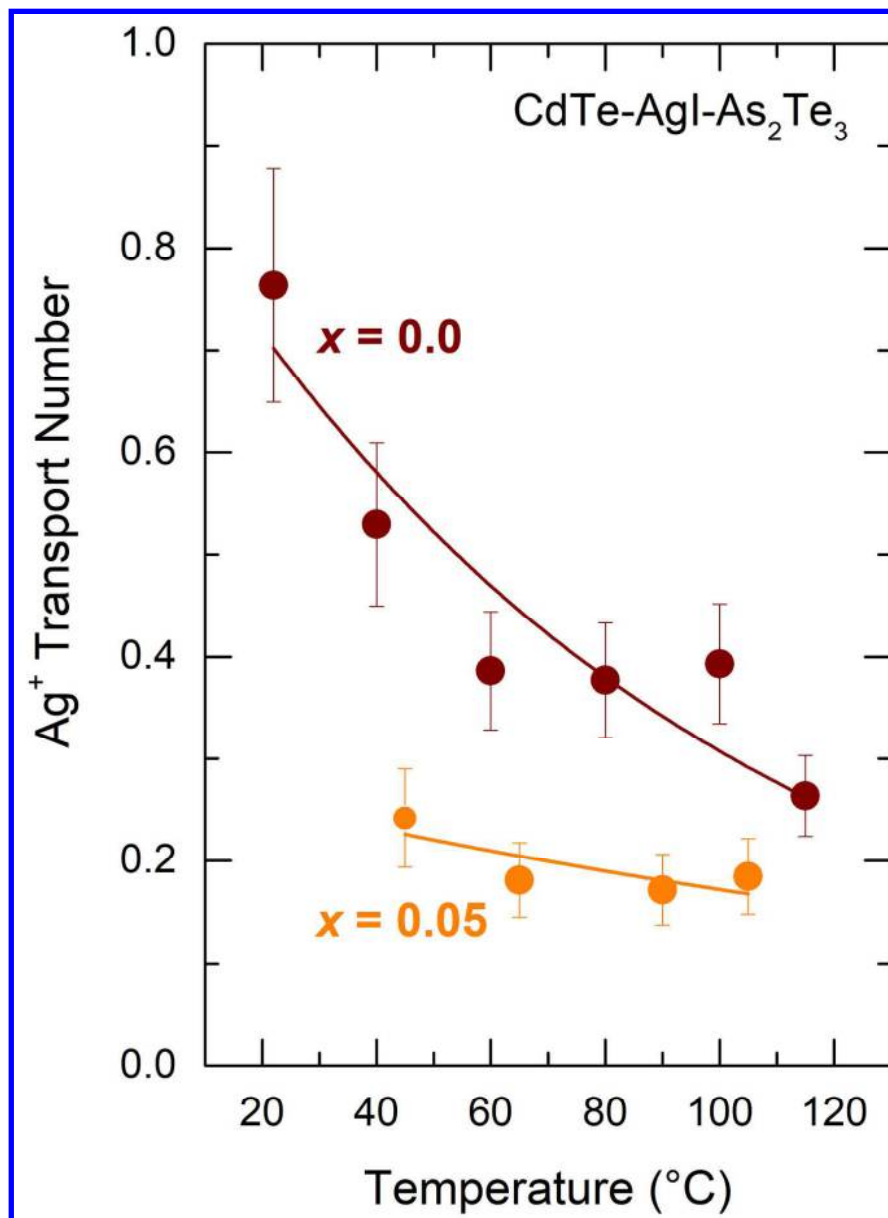


Figure 5. Total conductivity σ_{dc} and ionic transport parameters for the ternary CdTe-AgI-As₂Te₃ glasses: (a) room-temperature σ_{dc} and $H_R \sigma_{Ag^+}$; (b) the conductivity E_σ and diffusion E_d activation energies, and (c) the conductivity σ_0 and recalculated diffusion $H_R \sigma_0(Ag^+)$ pre-exponential factors. All solid lines are a guide to the eye.

230x152mm (150 x 150 DPI)



45 Figure 6. Silver ion transport number t_{Ag^+} plotted as a function of temperature for selected $(\text{CdTe})_x(\text{AgI})_{0.5-x/2}(\text{As}_2\text{Te}_3)_{0.5-x/2}$ glasses, $x = 0$ and 0.05 .

48 183x250mm (300 x 300 DPI)

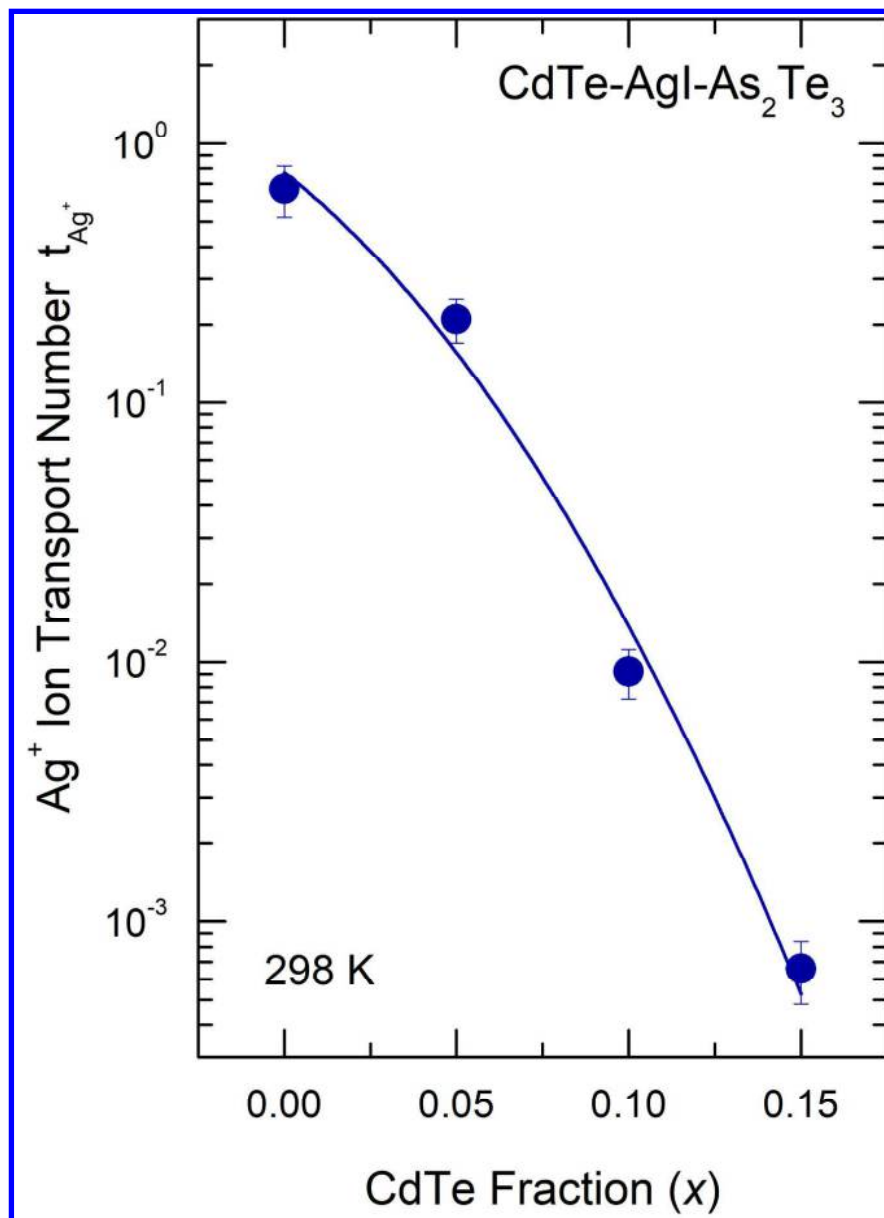


Figure 7. Room temperature silver ion transport number t_{Ag^+} for the ternary $(\text{CdTe})_x(\text{AgI})_{0.5-x/2}(\text{As}_2\text{Te}_3)_{0.5-x/2}$ glasses plotted as a function of CdTe content.

174x239mm (300 x 300 DPI)

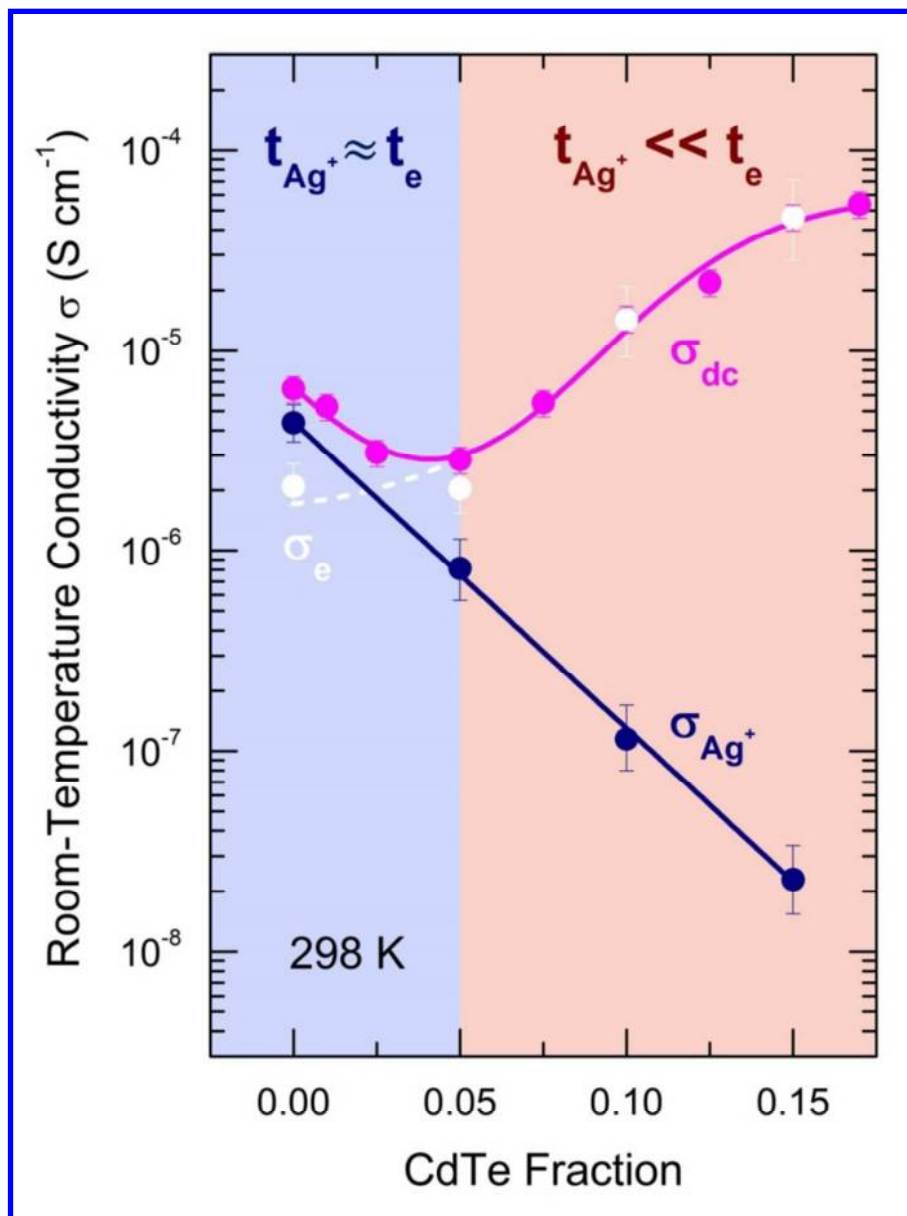


Figure 8. Room temperature total conductivity σ_{dc} as well as its ionic σ_{Ag^+} and electronic σ_e components for the ternary CdTe-AgI-As₂Te₃ glasses.

97x129mm (220 x 220 DPI)

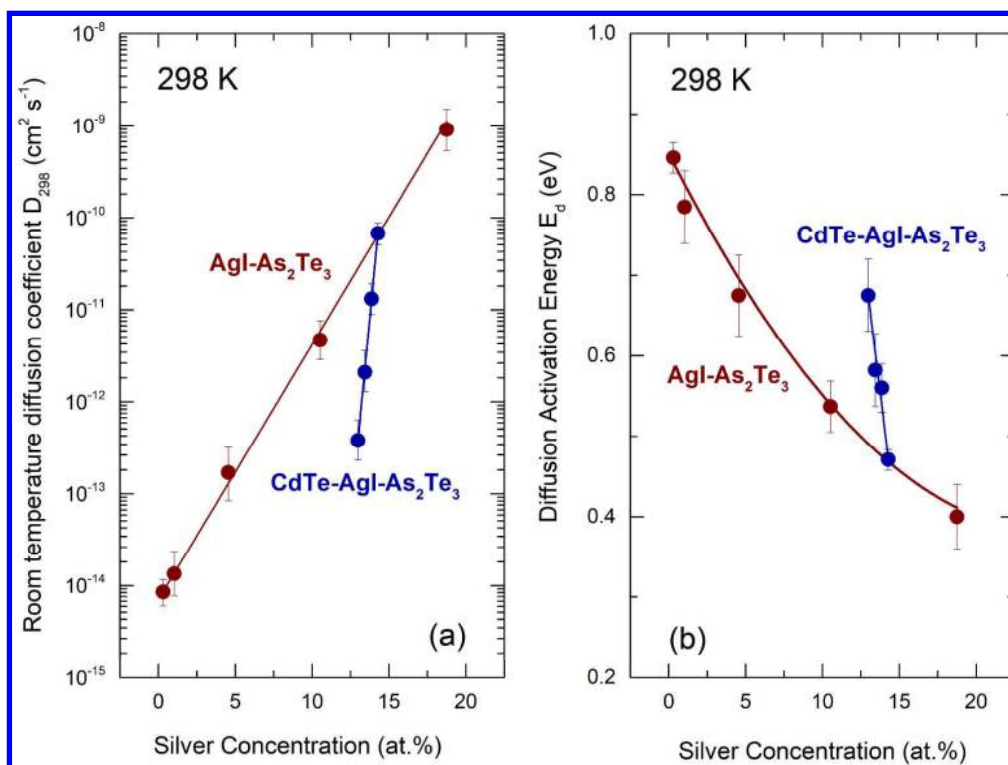


Figure 9. (a) Room temperature diffusion coefficient D_{Ag} , and (b) diffusion activation energy E_d for the binary AgI-As₂Te₃¹⁷ and ternary CdTe-AgI-As₂Te₃ glasses plotted as a function of the silver content. The solid lines are drawn as a guide to the eye.

410x306mm (300 x 300 DPI)

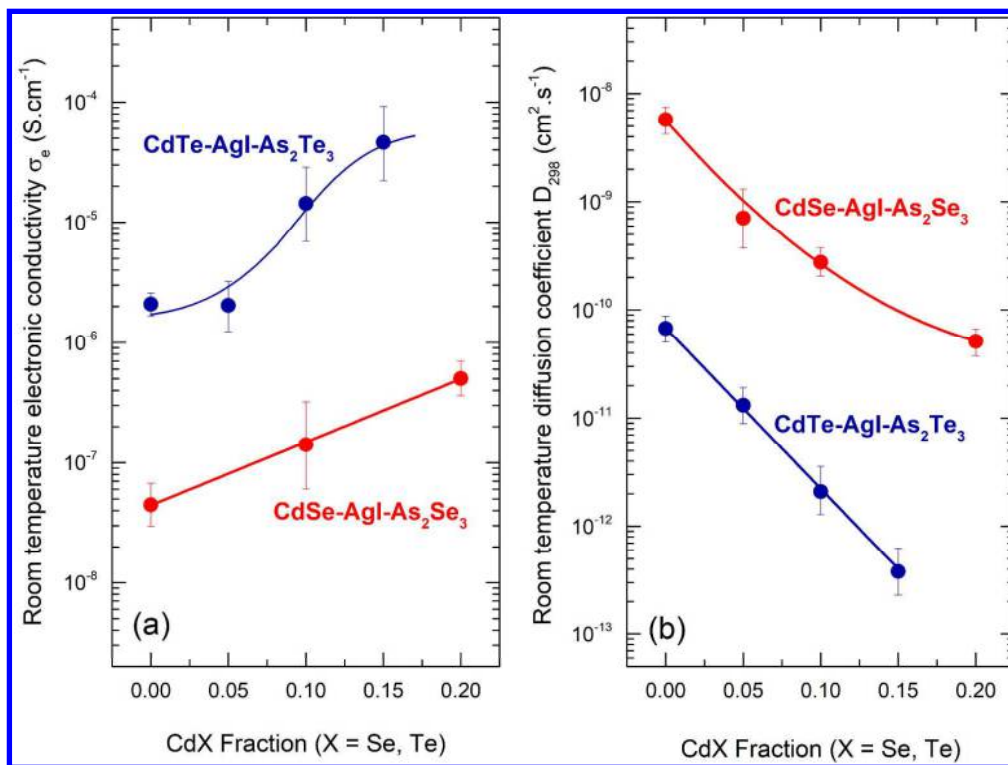


Figure 10. Room-temperature transport characteristics of the ternary $(\text{CdX})_x(\text{AgI})_{0.5-x/2}(\text{As}_2\text{X}_3)_{0.5-x/2}$ glasses, where X = Se or Te: (a) electronic conductivity; (b) ^{110m}Ag tracer diffusion coefficient.

407x304mm (300 x 300 DPI)